67º congresso 2012 abm
67th abm international congress
ISSN 1516-392X

ANALYSIS OF COMBINED ELECTRODES-ELECTROLYTE CERAMICS FOR HIGH AND INTERMEDIATE TEMPERATURE SOLID OXIDE FUEL CELLS[1]

José Geraldo de Melo Furtado[2]

Abstract

Solid oxide fuel cell (SOFC) is the more efficient electrical power generator known and it is typically composed an oxygen ion electrolyte and ceramic electrodes constituting a combined electrodes-electrolyte ceramic (CEEC) device, which is the heart of the SOFC, where charge and mass transfer processes occur that give rise to electrothermal behavior of the device. However, these processes are determined by the micro and nanostructural features of the CEEC and its interfaces. In this sense, this work aims to characterize and evaluate the structural characteristic of CEEC with main focus on the analysis performed by microscopy techniques, X-ray diffraction and fluorescence analysis. Structural and compositional analysis results were compared with the electrothermal characterization made by impedance spectroscopy. The results show the importance of uniformity of porous electrodes, high densification level and physical-chemical homogeneity of the electrolyte to the macroscopic electric performance of the device. The influence of bulk, interface and surface physical-chemical characteristics were analyzed and discussed. The best results in terms of ionic and electrical conductivities are in the range 0.03 to 0.1 S/cm at a temperature range from 650 to 900^{0}C.

Key words: Fuel cells; Solid oxide fuel cell; Solid electrolyte; Electrolyte-electrode assembly.

ANÁLISE DE CONJUGADOS CERÂMICOS ELETRODOS-ELETRÓLITO PARA CÉLULAS A COMBUSTÍVEL DE ÓXIDO SÓLIDO

Resumo

Célula a combustível de óxido sólido (SOFC) é o mais eficiente gerador de energia conhecido, sendo composto por um eletrólito e dois eletrodos cerâmicos constituindo um conjugado cerâmico eletrodo-eletrólitos (CEE), que é o coração da SOFC, no qual os processos de transferência de massa e de carga ocorrem e dão origem ao comportamento eletrotérmico do dispositivo. No entanto, estes processos são determinados pelas características micro e nanoestruturais do CEE e das respectivas interfaces em jogo. Neste sentido, este trabalho tem por objetivo caracterizar e avaliar as característica estruturais de CEEs com foco principal na análise realizada por técnicas de microscopia, difração de raios-X e análise de fluorescência. Os resultados da análise estrutural e de composição foram comparados com a caracterização electrotérmica feita por espectroscopia de impedância. Os resultados mostram a importância da uniformidade dos eletrodos porosos, do elevado nível de densificação e da homogeneidade físico-química do eletrólito para o desempenho elétrico macroscópico do dispositivo. A influência das características físico-químicas interfaciais e superficiais, além das massivas, foram analisadas e discutidas. Os melhores resultados, em termos de condutividades iónica e elétrica, estão no intervalo de 0,03 a 0,1 S/cm, numa faixa de temperaturas de 650 a 900^{0}C.

Palavras-chave: Células a combustível; SOFC; Eletrólito sólido; Conjugado eletrólito-eletrodos.

[1] *Technical contribution to 67th ABM International Congress, July, 31th to August 3rd, 2012, Rio de Janeiro, RJ, Brazil.*

[2] *D.Sc., Researcher, Special Technologies Department (DTE), Electric Power Research Center, Cepel, P.O.Box 68007, 21940-970, Rio de Janeiro, Brazil. e-mail: furtado@cepel.br*

ISSN 1516-392X

1 INTRODUCTION

Fuel cells are electrochemical devices that, via electrochemical reactions, are able to combine a fuel and an oxidant, converting the stored chemical energy of the fuel directly into direct-current electrical energy and heat as a byproduct. The fuel is not burned (there is no combustion), such as in a flame, as in conventional power generation systems; rather, it is electrochemically oxidized. Thus, the maximum efficiency of a fuel cell is not limited by the Carnot cycle, which limits many conventional power systems such as the internal combustion engines, steam and gas turbines, and heat pumps.[1] Thus, fuel cells have been regarded as the main power generation equipment capable of increasing the energy conversion efficiency and reduce or eliminate the emission of pollutants in various fields of applications. [2,3]

Solid oxide fuel cell (SOFC), one of the types of fuel cells, is one of the most promising technologies for the production of energy, with potential to be a typical future distributed cogeneration system[4,5] due to it high energy efficiency, low pollutant emissions, potential fuel flexibility, high modularity as a solid-state device and co-generation capability.[5,6] Typically, a SOFC system is constituted of at least seven distinct components:[6-8] fuel feed, anode, electrolyte media (separating the two electrodes), cathode, oxidant agent feed (normally air), sealing materials and electrical interconnectors (completing the electrical circuit) as schematically showed in the Figure 1.

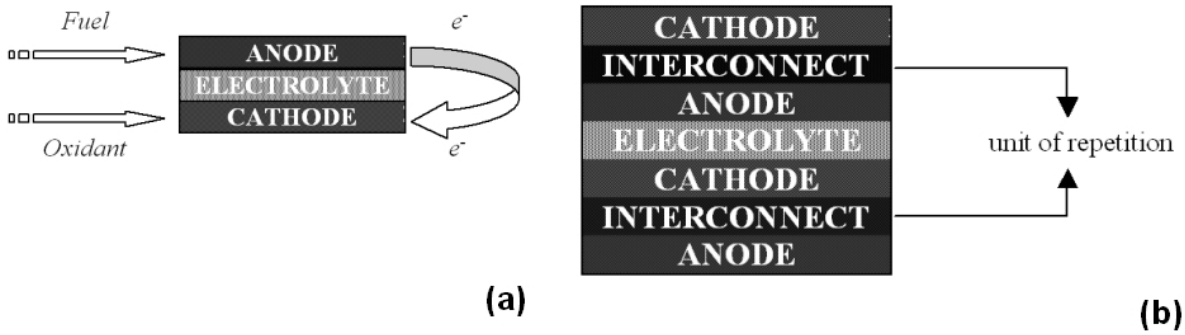

Figure 1. (a) Schematic diagram of a fuel cell; (b) scheme of the connection of the anode of a single fuel cell to the cathode of the subsequent single fuel cell, constituting a solid oxide fuel cell stack.

In SOFC technology, the heart of the fuel cell is a solid-state composite material-device of which emerges the respective electrical fuel cell behavior. This composite component is the Electrolyte-Electrodes Assembly (EEA), also known as MEA (Membrane Electrode Assembly), which is composed by a solid electrolyte sandwiched by two electrocatalysts-porous-electrodes, becoming the main component that holding the most significant influence on overall cost, useful life and fuel cell performance. [8-10] Technologically there is a greater tendency to develop the planar configuration for SOFC systems, and this type of configuration is capable of achieving very high power density,[8,11] characterized by a very thin electrolyte deposited on an anode considerably thicker, but that presents a reaction zone typically five to six times thicker than the electrolyte.[6,11] Thus, the electrolyte contribution to the ohmic loss is minimized and the microstructural characteristics of the interfacial electrolyte/anode region become highly relevant to determining the electrical behavior of SOFC. Accordingly, this work aims to characterize and evaluate the structural characteristic of combined electrodes-electrolyte ceramic (CEEC) with main focus on the analysis performed by microscopy techniques, X-ray diffraction

ISSN 1516-392X

and fluorescence analysis, within a research line of the CEPEL (Electric Power Research Center, Brazil), as a contribution to the characterization and understanding of the behaviour of these systems.

2 EXPERIMENTAL

In this work studies were performed with systems electrolyte/anode 8YSZ/Ni-YSZ and ERC/NiO, where ERC is rare-earth-doped ceria (RedCe) and 8YSZ is yttria-(8mol%)-stabilized zirconia, which are the electrolytes that have been considered for SOFC applications of high and intermediate temperature. The respective ceramic electrolyte powders were synthesized and applied to the anode structures.
For the synthesis of 8mol%Y_2O_3-stabilized zirconia (8YSZ) powder, by Pechini's method, the zirconium oxychloride octahydrate ($ZrOCl_2.8H_2O$) and the yttrium nitrate pentahydrate ($Y(NO_3)_3.5H_2O$) were dissolved in ethylene glycol, anhydrous citric acid was added in a molar ratio of 1:5 between ethylene glycol and citric acid. The mixture was stirred for about 30 minutes under heating to 80°C, to promote polyesterification. The resulting gel was kept in oven at 180°C for 12 hours. The resulting fine powders were calcined at 900°C for 6h using heating rates of 10°C/min, with air flow rate of 60 mL/min. The ERC system was obtained from acid digestion of praseodymium, dysprosium and yttrium oxides under stirring at 70^0C for 48 hours and subsequent them infiltration into the matrix of ceria powder, heated to 120^0C and stirring for 24 hours. Suspensions of the respective powders were prepared and deposited by tape casting (8YSZ) and by filtering (ERC) on the respective anode materials. The systems were sintered and prepared for characterization. Figure 2 schematically shows the processes of preparation and characterization.

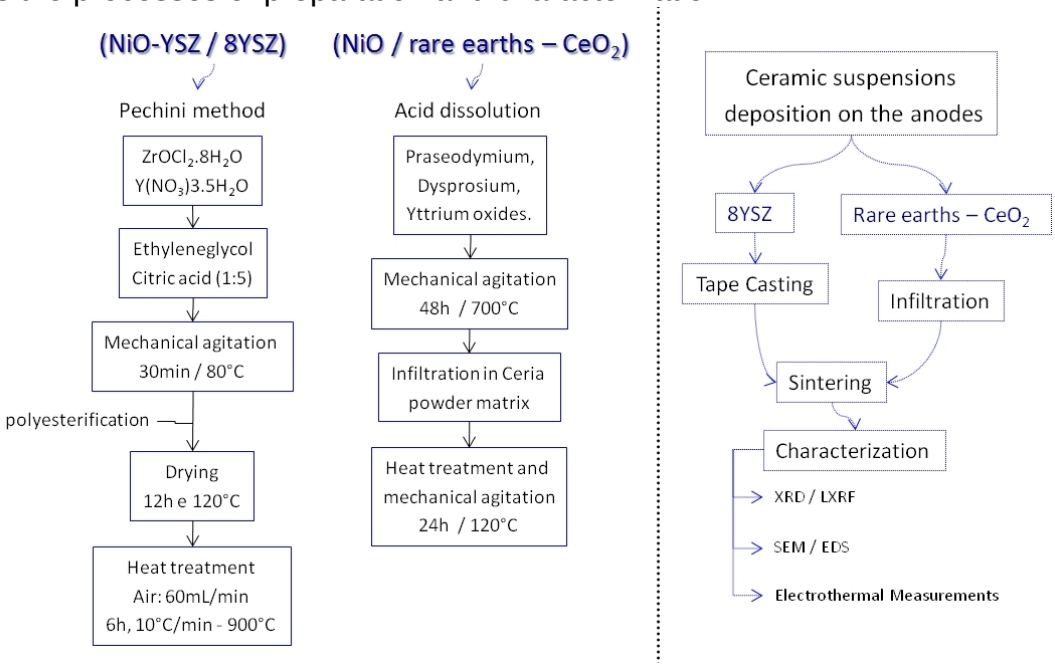

Figure 2. Schematic representation of the methods of preparation and characterization used in this work.

Crystalline phases were detected by X-ray diffraction (XRD) analysis with a PANalytical X'Pert PRO diffractometer using Cu Kα-radiation (λ = 1.541806Å) with Ni filter and the data were collected from 20° to 100°. The microstructures of the

ISSN 1516-392X

samples were examined by scanning electron microscopy (SEM, Jeol JSM-64602 LV) equipped with X-ray dispersive energy spectroscopy (EDS, Link ISIS, Oxford Instruments) for chemical compositional analysis and by local x-ray fluorescence analysis (LXRF 40 kV, SMACo). The electrothermal behavior was measured using a curve tracer source-measurement unit (Tektronix 577) and an Agilent 4294A precision impedance analyzer.

3 RESULTS AND DISCUSSION

Figures 3(a) and 3(b) show photomicrographs of the 8YSZ/Ni-YSZ combined anode electrode-electrolyte ceramic and an EDS spectrum (Fig. 3(c)). Both in the Figure 3(a) as in Figure 3(b) it were clearly identifies the regions of the electrolyte and of the anode as a function of their characteristic aspects of the consolidated materials are very different, since the anode is essentially porous, while the electrolyte is essentially dense. In fact, according to the photomicrograph shown in Figure 3(b) it was observed the porous structure of anode and electrolyte microstructures showing clear grain boundaries as a result of high densification, although intra- and mainly intergranular pores are observed, which can be reduced or eliminated by optimizing the sintering. In Figure 3(a), secondary electrons image, it was note the dimensions involved and, in this case, the thickness of electrolyte is about twenty times lower than that of the anode. The microstructural characteristics of the interface electrolyte/anode can also be examined from the photomicrograph of Figure 3(b), backscattered electrons image, in which it appears that although there is some heterogeneity, there was no interpenetration between the layers. Figure 3(c) shows the EDS spectrum characteristic of ceramic combined system shown in Figure 3(a), showing, as expected, only the presence of Zr, Y and Ni.

ISSN 1516-392X

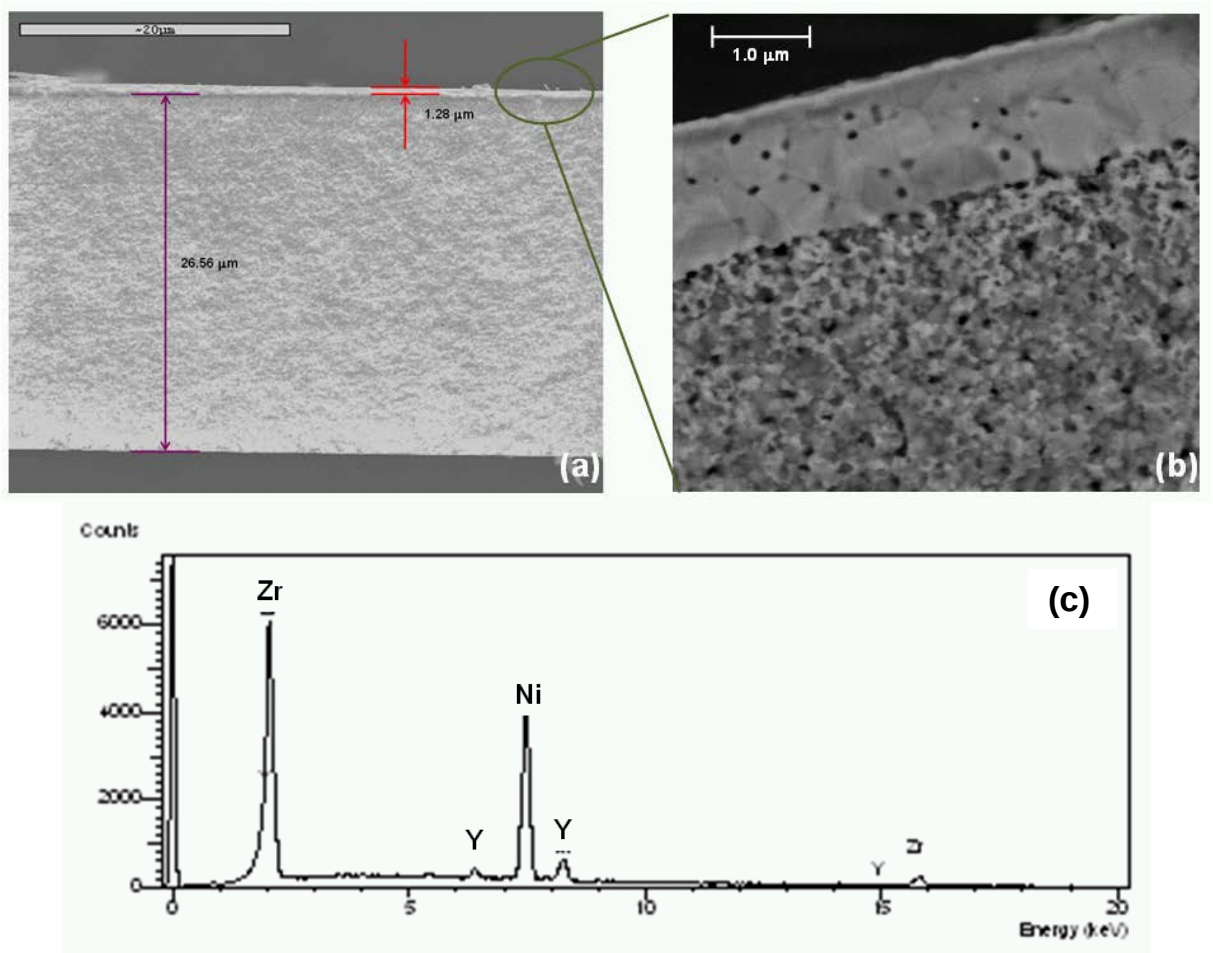

Figure 3. SEM photomicrographs: (a) secondary electrons image - 8YSZ/Ni-YSZ combined anode electrode-electrolyte ceramic sample; (b) backscattered electrons image - amplified region showing the 8YSZ/Ni-YSZ interface and the anode reaction zone. (c) X-ray dispersive energy spectroscopy (EDS) spectrum characteristic of ceramic combined system shown in Figure 3(a).

The results of a detailed profiles EDS microanalysis can be seen in Figure 4, where the composition is chemically analyzed along the yellow line shown on the photomicrography and beginning at a point located within the grain of 8YSZ and ends in the anodic region already distant of the 8YSZ/electrode interface, but yet the typical reaction zone (porous anode structure). The EDS spectra along said line, for the elements Zr, Y and Ni are shown respectively in Figures 4(b), 4(c) and 4(d) and the results indicate the absence of interpenetration, since Ni essentially it was not detected in the area of the electrolyte (Figure 4d), which presents a partially complementary to the profile of Zr (Figure 4b). After the interface electrolyte/electrode count on Ni is considerably high and, based on the image obtained with backscattered electrons (Figure 4a) it was noted that the Ni is well dispersed in the reaction zone. On the other hand, the Y has a profile of amphoteric character, since it is found at comparable levels (slightly higher in the area of the electrolyte) on both sides of the interface electrolyte/anode. The absence of interpenetration of Ni is an indication of suitable conditions of processing, but still need some optimization in order to reduce the porosity remaining in the electrolyte, because on the one hand, as noted by Nakajo et al.[12] the diffusion of Ni into the electrolyte can lead to failures of SOFC at high temperatures and, on the other hand, porosity is a factor that results in loss of efficiency of the electrolyte.[6,10]

ISSN 1516-392X

In a complementary manner and also on the chemical analysis Table 1 presents results of local X-ray fluorescence analysis related to the areas bounded by colored squares that appear in Figure 4(a). As can be seen by the numerical results of the table, the red square area has a typical chemical composition of a YSZ ceramic, while the green and white square areas are related to the elementary chemical compositions of the anode structure, showing a still more significant presence of nickel (of the order of twice) in the area closest to the electrolyte (green square) and, therefore, where there is a greater degree oxidation of fuel. Also in this case, the concentration of yttrium is higher, indicating a global basis, greater effectiveness in that area of TPR. As for the blue square representing an area that includes the interface electrolyte/anode, there is a reduction of approximately 28% at a concentration of Y in relation to the core of the electrolyte, as well as a Ni concentration of about ten times smaller that this feature of the green square. An increase of this concentration could result in an improvement of electrothermal and electrochemical performance of the device.

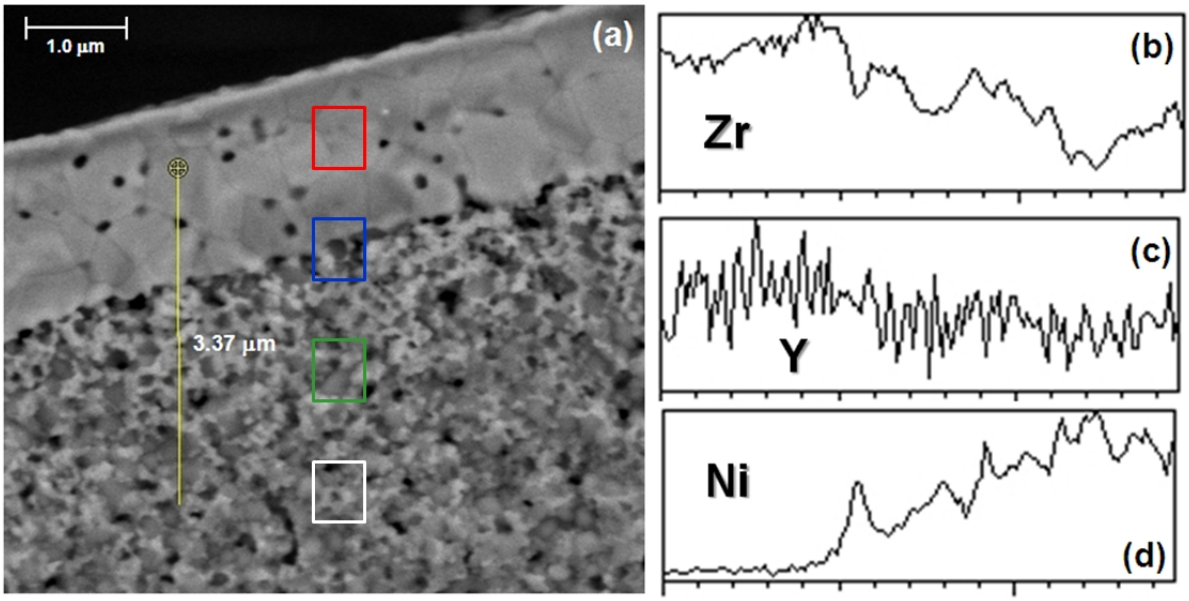

Figure 4. SEM-EDS Analysis: (a) backscattered electrons image - amplified region (Figure 3(b)) showing the 8YSZ/Ni-YSZ interface and the anode reaction zone, as well as the yellow line where EDS analysis was carried out; EDS spectrum for (b) Zr, (c) Y, and (d) Ni. Colored squares shown in 3(a) limit the areas investigated by LXRF analysis.

Table 1. Local X-ray fluorescence results of the analysis of the microstructure shown in Figuew 4(a)

Square Region *(in Fig. 3(a))*	Composition: Average content of elements (wt %)		
	Zr	**Y**	**Ni**
red	87.4 ± 0.2	12.6 ± 0.5	0
blue	90.1 ± 0.1	9.1 ± 0.3	0.8 ± 0.1
green	85.2 ± 0.5	7.2 ± 0.3	7.6 ± 1.8
white	89.3 ± 0.2	5.9 ± 0.4	4.8 ± 0.8

The microstructure of the anode can also be best seen in the photomicrographs shown in Figure 5, which show the porous nature of the structure, which is essential to ensure the percolation and diffusion of gas and the establishment of the triple-phase region (TPR) [6], still providing thermal stability to the device.[13]

In fact, the characteristics of the transition region between the porous anode and dense electrolyte that ultimately characterize the interface 8YSZ/Ni-YSZ, are critical

ISSN 1516-392X

to ensure performance and stability for a SOFC.[12,13] It should ensure that there is electrical connection available for ionic transport in this interface, without the existence of discontinuities that result in the establishment of impedances.[6,14] In this sense, the high densification of the electrolyte is essential.[12,15,16] Particularly in the photomicrographs of Figure 6 to identify clear grain boundaries, although in Figure 6(a) it is possible to identify any inter-and intragranular porosity, as seen in Figures 3(b) and 4(a). Since Figure 6(b) shows the absence of porosity and average grain size slightly less than the characteristic of Figure 6(a). The EDS spectrum shown in Figure 6(c) is associated with the photomicrograph of Figure 6(b) and indicates, as expected, only the elemental composition of the electrolyte, without contamination by Ni.

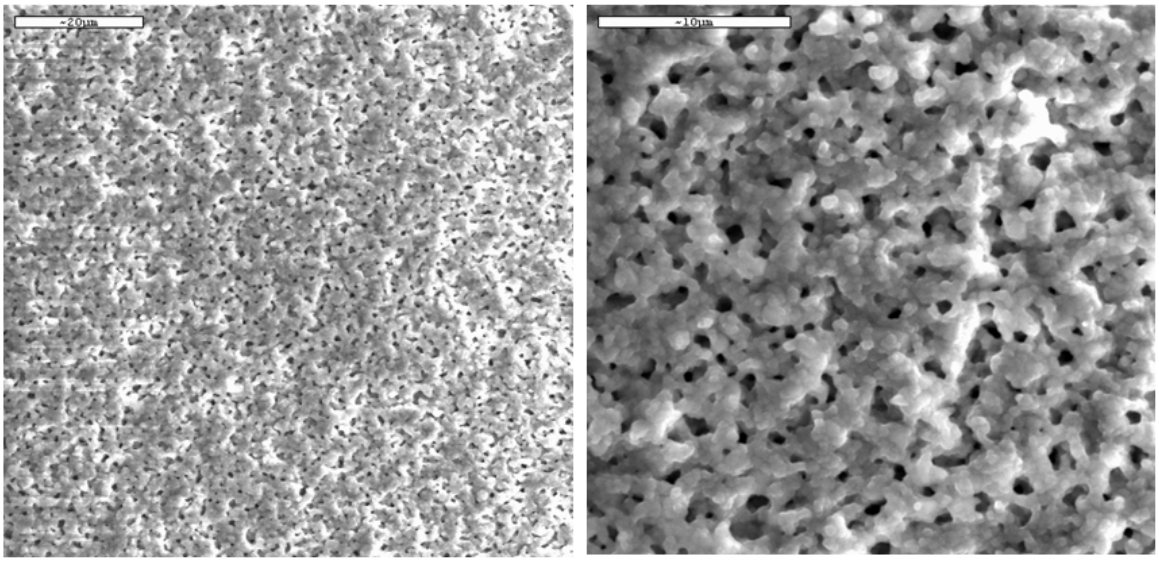

Figure 5. SEM photomicrographs (secondary electrons image) of the anodic electrode of the 8YSZ/Ni-YSZ combined electrodes-electrolyte ceramic.

In researches that have been developed in Cepel the focus has been the characterization and evaluation of electrolytes and electrode / electrolyte interface, as well as studies of processing to obtain highly densified electrolyte as shown in the photomicrographs of Figures 6(b), 7(a) and 7(b). To mount the unit cells have been used commercial cathode, which like the anode must have porous structure. Figure 7(c) shows a typical photomicrograph of the microstructure of SOFC cathodes.

ISSN 1516-392X

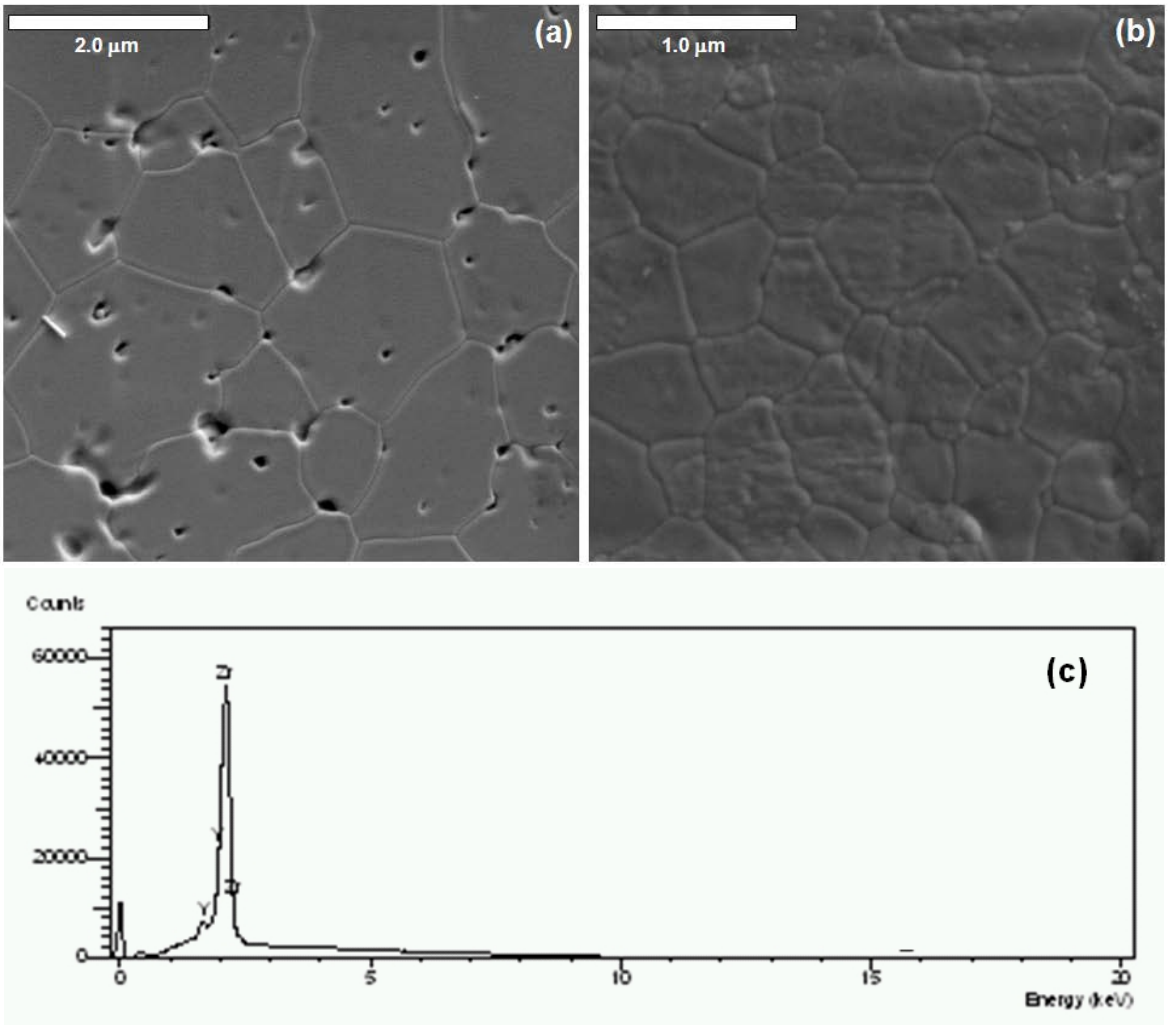

Figure 6. SEM micrographs of 8YSZ specimens sintered in different conditions: (a) showing mainly intergranular porosity; (b) showing a fully densified microstructure; (c) overall characteristic EDS spectrum.

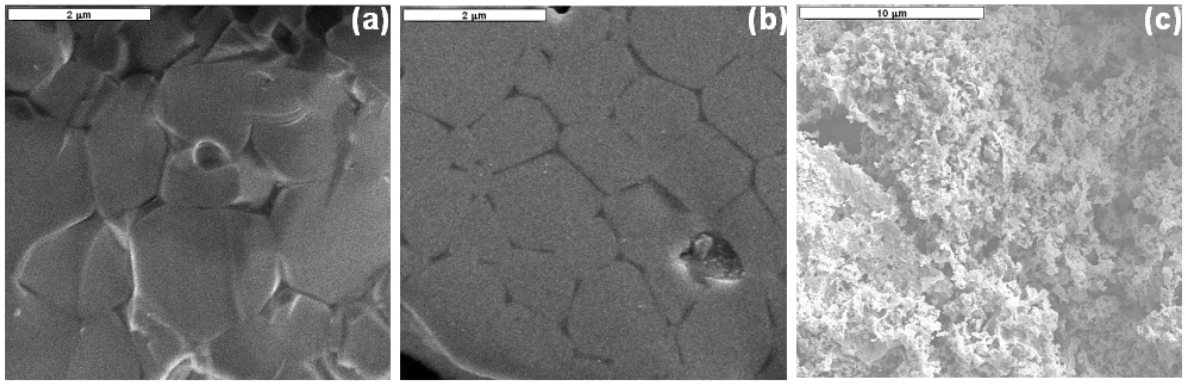

Figure 7. SOFC material microstructures: (a) and (b) full-densified YSZ ceramic; (c) porosity cathode ceramic.

Besides the traditional 8YSZ electrolyte, we have been also worked with electrolyte in the production of alternative combined electrode-electrolyte for application in intermediate temperature SOFC (IT-SOFC). Figure 8 shows a photomicrograph of the microstructure of a combined ERC/NiO and its chemical analysis by EDS of the

ISSN 1516-392X

electrolyte layer. The microstructure shows a distribution of porosity increasing from top to bottom, once the top layer is the electrolyte.

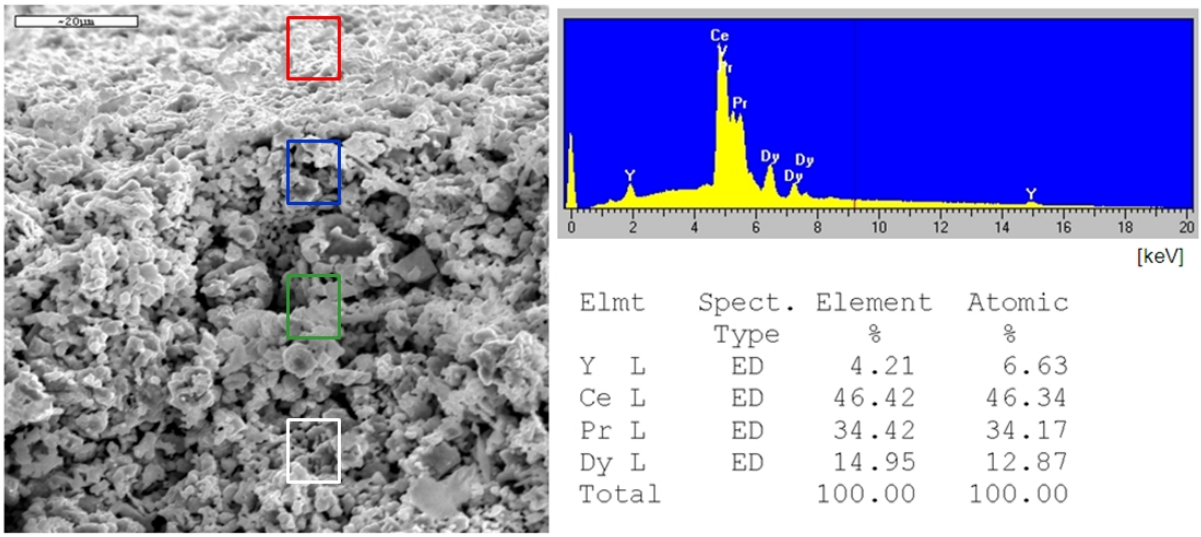

Figure 8. SEM micrographs of ERC/NiO combined bilayer and electrolyte layer characteristic EDS spectrum. Colored squares shown in the photomicrograph limit the areas investigated by LXRF analysis.

Likewise as shown in Table 1 and Figure 4, Table 2 presents the results of local X-ray fluorescence analysis related to the areas bounded by colored squares that appear in Figure 8. Although not detected the presence of nickel in the upper layer of the electrolyte, the results in Table 2 do not show a differentiation compositional well established to that emerges from the results shown in Table 1. In fact, for example, there is little difference in the levels of rare-earths along the thickness of the device. Certainly this aspect is related to the infiltration process of dopants in the array of ceria, which still is in improvement.

Table 2. Local X-ray fluorescence results of the analysis of the microstructure shown in Fig. 8.

Square Region *(in Fig. 7)*	Composition: Average content of elements (wt %)				
	Ce	**Y**	**Pr**	**Dy**	**Ni**
red	82.6 ± 0.4	1.2 ± 0.4	3.4 ± 0.6	2.8 ± 0.2	0
blue	80.4 ± 0.4	1.0 ± 0.6	4.6 ± 0.4	3.0 ± 0.8	1.0 ± 0.3
green	80.2 ± 0.6	3.2 ± 0.8	6.7 ± 0.6	4.2 ± 0.8	5.7 ± 2.0
white	86.3 ± 1.2	1.0 ± 0.5	6.1 ± 0.8	2.6 ± 0.5	4.0 ± 1.2

Figure 9 shows the X-ray diffraction patterns of the two electrolytes synthesized in this work and used in the preparation of the respective combined electrodes-electrolyte ceramics. For 8YSZ sample are identified characteristic peaks of cubic fluorite type structure and for the sample RedCe the peaks are characteristic of the solid solution of ceria and yttria doped with praseodymium (0.144 mol) and dysprosium (0.346 mol).

ISSN 1516-392X

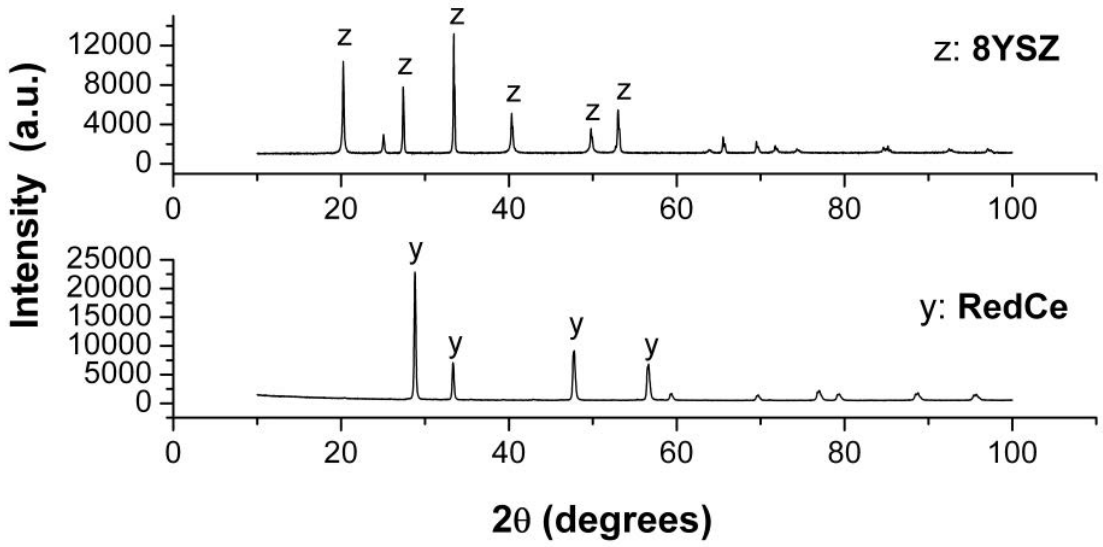

Figure 9. X-ray diffraction patterns of the studied electrolyte ceramics.

Figure 10 shows the results of ionic conductivity of both electrolytes studied as well as the results of total electrical conductivity of the combined electrode-electrolyte ceramics evaluated.

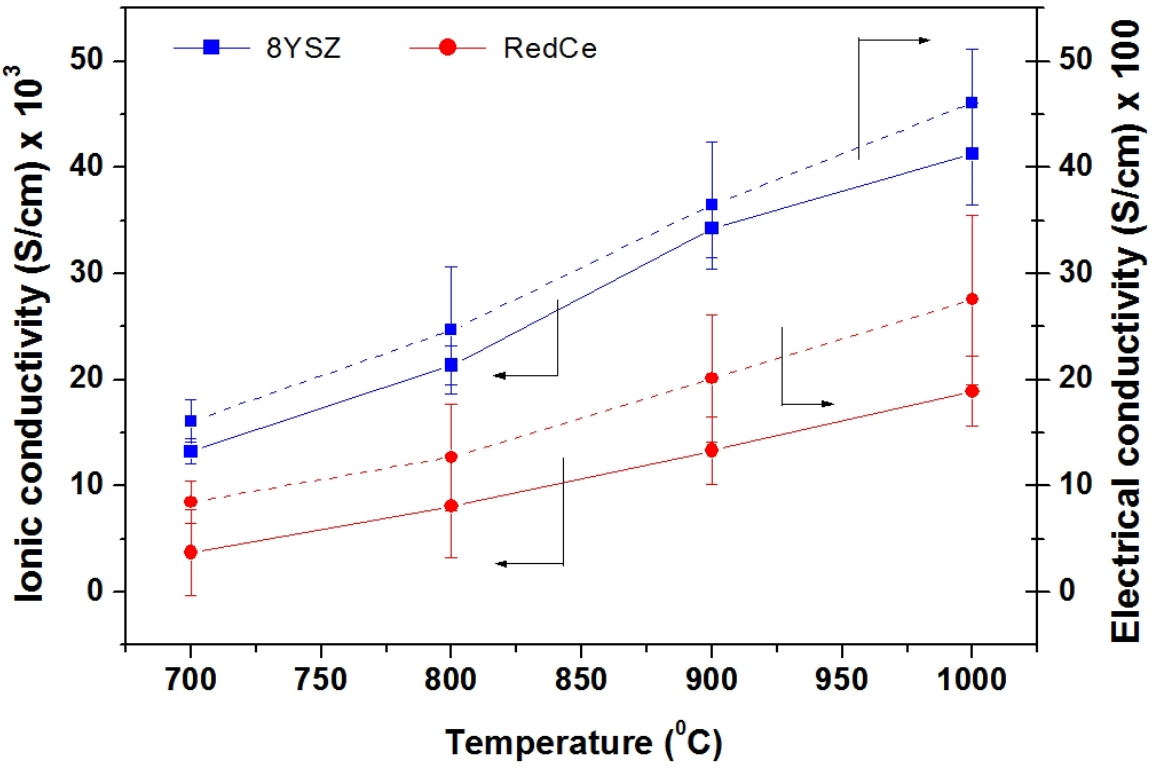

Figure 10. Ionic conductivity (solid lines read on the left axis) and total electrical conductivity (dashed lines read on the right axis) of the electrolyte combined ceramics studied as a function of temperature in the range of 700 to 1000^{0}C.

These electrothermal characterization results (Figure 10) show that the difference in ionic conductivity between the two electrolytes is higher mainly for temperatures above 850^{0}C, although, for the case studied, the ionic conductivity of 8YSZ are much

ISSN 1516-392X

larger along the entire temperature range, which is certainly a reflection of their greater degree of densification, since the samples based on ceria could not reach the same level of densification. This also seems to be responsible for the variability of the values of ionic conductivity of ceria electrolyte.
In fact, this behavior is also similar to the total electrical conductivity of the conjugate also shown in Figure 10. In this case, the relative difference is smaller, but the variability is significant, particularly for the system ERC/NiO. As can be seen by comparing the microstructures shown in Figures 3 and 8 this latter system provides greater porosity and microstructural heterogeneity, which were reflected on its electrical characteristics, contributing greatly to the reduction of transport properties of electric charge. These observations are also in agreement with the compositional results shown in Tables 1 and 2, which shows a better condition to set a larger area of TPR on the system based on YSZ. The fact that the system ERC/NiO has been produced by the filtration technique, due to its microstructure, shows that this process is not yet optimized, which incidentally also occurs, although to a lesser extent, with the production system 8YSZ/Ni by tape casting. Indeed, studies have now developed aimed at improving production techniques of these combined electrodes-electrolyte ceramics.

4 CONCLUSIONS

This work presented results of microstructural, chemical compositional and electrical characterization of combined electrodes-electrolyte ceramics for application in solid oxide fuel cells. The main objective of the research with theses materials and devices is to produce more homogeneous and full densified electrolyte ceramic microstructure and electrodes with uniformly distributed porosity and high electrocatalytic activity, which will result in fuel cells with better electrical performance and higher electrothermal stability, thereby enabling the reduction of the operating temperature of such fuel cell type. Accordingly, were produced and characterized combined electrodes-electrolyte by tape casting and filtration method. The results showed the establishment of 8YSZ-Ni interface and anodic reaction zone conditions that suggests by microstructural evaluation be very close to the adequate, which is corroborated by the results of electrothermal characterization. Moreover, obtaining CER/NiO conjugate was more difficult and process improvements should be implemented in the future.

REFERENCES

1 FAGHRI, A. Unresolved Issues in Fuel Cell Modeling. **Heat Transfer Engineering**, v.27, p. 1-3, 2006.
2 HOFFERT, M. I. Energy implications of future stabilization of atmospheric CO_2 content. **Nature**, v.395, p. 881-884, 1998.
3 CRABTREE, G. W., DRESSELHAUS, M. S., BUCHANAN, M. V. The Hydrogen Economy. **Physics Today**, Dec, 2004.
4 4. NEEF, H.-J. International overview of hydrogen and fuel cell research. **Energy**, V. 34, p. 327-333, March 2009.
5 ZINK, F., LU, Y., SCHAEFER, L. A solid oxide fuel cell system for buildings. **Energy Conversion and Management**, V. 48, p. 809-818, March 2007.

ISSN 1516-392X

6 MINH, N. Q. Solid Oxide Fuel Cell Technology-Features and Applications, **Solid State Ionics**, v. 174. p. 271-277, 2004.
7 WINCEWICZ, K. C., COOPER, J. S. Taxonomies of SOFC material and manufacturing alternatives. **Journal of Power Sources**, 140, p.280-296, 2005.
8 SINGHAL, S. C., KENDALL, K. High temperature Solid Oxide Fuel Cells: Fundamentals, Design and Applications, Oxford, UK: Elsevier Ltd., p. 405, 2003.
9 IVERS-TIFFÉE, E., et al. Macroscale modeling of cathode formation in SOFC. **Solid State Ionics**, v.174, n.1-4, p. 223-232, 2004.
10 STEELE, B. C. H., HEINZEL, A. Materials for fuel-cell technologies. **Nature**, v.414, p. 345-352, 2001.
11 HUSSAIN, M. M., LI, X., DINCER, I. A general electrolyte–electrode-assembly model for the performance characteristics of planar anode-supported solid oxide fuel cells. **Journal of Power Sources**, 189, p.916-928, 2009.
12 NAKAJO, A., et al. Simulation of thermal stresses in anode-supported solid oxide fuel cell stacks - Part I: Probability of failure of the cells. **Journal of Power Sources**, 193, p. 203–215, 2009.
13 PIHLATIE, M., KAISER, A., MOGENSEN, M. Redox stability of SOFC: Thermal analysis of Ni–YSZ composites. **Solid State Ionics**, v.180, n.17-19, p.1100-1112, 2009.
14 LAURENCIN, J., et al. Impact of ‘redox’ cycles on performances of solid oxide fuel cells: Case of the electrolyte supported cells. **Journal of Power Sources**, v.195, n.9, p.2747-2753, 2010.
15 PÉREZ-COLL, D., SÁNCHEZ-LÓPEZ, E., MATHER, G. C. Influence of porosity on the bulk and grain-boundary electrical properties of Gd-doped ceria. **Solid State Ionics**, v.181, n. 21-22, p. 1033-1042, 2010.
16 LIU, Y.L., et al. Microstructural studies on degradation of interface between LSM–YSZ cathode and YSZ electrolyte in SOFCs. **Solid State Ionics**, v.180, n. 23-25, p. 1298-1304, 2009.